EXTENDED REPORT

Accuracy of quantitative magnetic resonance imaging in the detection of ex vivo focal cartilage defects

H Graichen, D Al-Shamari, S Hinterwimmer, R von Eisenhart-Rothe, T Vogl, F Eckstein

Ann Rheum Dis 2005;**64**:1120–1125. doi: 10.1136/ard.2004.029678

See end of article for authors' affiliations

Correspondence to: Dr H Graichen, Research Group for Kinematics and Biomechanics, Orthopedic Department, University of Frankfurt, Marienburgstr, 2, 60528 Frankfurt, Germany; h.graichen@em.uni-frankfurt.de

Accepted 28 December 2004
Published Online First 7 January 2005

Background: No established, non-invasive diagnostic procedure for quantifying focal cartilage defects is currently available.
Objective: To test the accuracy of quantitative magnetic resonance imaging (qMRI) for reliable determination of cartilage defect size in various compartments of the human knee.
Methods: 24 tibial and patellar cartilage plates were harvested during knee arthroplasty. 74 cylindrical defects with diameters of 3, 5, and 8 mm were created with a punch. In 15 specimens (51 defects), the cartilage cylinders (inside the punch) were removed (approach 1), while in 9 specimens (23 defects) the surrounding tissue was removed mechanically and the cartilage cylinder was left in place (approach 2). All plates were imaged with a T_1 weighted water excitation gradient echo sequence at a resolution of 1.5 mm×0.31 mm×0.31 mm. The defect size was computed from the image data after interactive segmentation and compared with the known dimensions of the cylinders.
Results: Although there was a significant overestimation of the defect size by qMRI in 3 mm defects (mean (SD) +1.3 (0.58) mm = ±42%; $p<0.001$), the overestimation was only +1.0 (0.57) mm (±21%; $p<0.05$) in 5 mm defects and +0.1 (0.39) mm (±4%; $p=0.31$) in 8 mm defects (approach 1). Values were similar for approaches 1 and 2 and for patellar and tibial cartilage plates.
Conclusions: These findings show that qMRI allows accurate quantification of focal cartilage defects. It may therefore represent a valuable tool in the diagnosis of traumatic cartilage lesions, osteochondrosis dissecans, and osteochondral fractures, and in monitoring their responsiveness to surgical or other treatments.

Up to 33% of American adults have symptoms of osteoarthritic (OA) cartilage lesions (press release from the Centers for Disease Control and Prevention, 24 October 2002). In particular, in young subjects, cartilage defects often do not affect the entire cartilage plate, but are confined to focal lesions. Focal alterations can also be observed in osteochondrosis dissecans and in acute osteochondral fractures.[1] In both these diseases the aim is to refill the defects with hyaline cartilage tissue, and new therapeutic approaches have recently been described (for example, autologous chondrocyte transplantation, mosaicplasty).[2–6] In this context, it would be highly beneficial to have a diagnostic method available for accurately estimating the defect size non-invasively preoperatively, without the need to subject the patient to an operative, arthroscopic procedure.

Follow up studies[2 6 7] have indicated good clinical results for the therapeutic approaches mentioned above, but arthroscopic (and histological) control examinations have shown that at least one third of the transplanted defects display persistent defects.[5 8 9] For these reasons, it would also be advantageous to use an accurate, postoperative technique which would allow measurement of the exact defect size non-invasively.

Conventional radiography has been the standard method for diagnosing OA[10] and focal cartilage defects.[11] However, this method cannot delineate cartilage directly, and does not allow determination of the size of focal cartilage defects.[12] Osteochondral and other cartilage lesions can now be described using magnetic resonance imaging (MRI),[13 14] and if the spatial resolution is sufficiently high focal cartilage defects can be detected with high reliability.[15 16]

We have recently shown that MRI, in conjunction with three dimensional image analysis techniques (qMRI), allows accurate measurement of cartilage loss in OA.[17 18] In this study we extend these techniques to quantify focal cartilage defects, and we analyse the accuracy of qMRI in measuring focal cartilage defects in different compartments of the knee experimentally.

MATERIALS AND METHODS

Specimens and creation of cartilage defects

Twenty tibial (medial and lateral) and 16 patellar joint surfaces (cartilage and subchondral bone) were harvested from human knees during knee arthroplasty. These were stored at −80°C and thawed to room temperature before each examination. In the 36 (20+16) joint surfaces, 74 cylindrical full thickness defects were artificially created with three different punches (Aesculap, Tuttlingen, Germany), with diameters of 3, 5, and 8 mm, respectively. Up to three defects were created in different areas of each tibial and patellar surface, both in areas with macroscopically intact cartilage and in areas with early OA changes. Note that the cartilage plates were retrieved from patients treated for femorotibial OA, but that substantial portions of normal cartilage and cartilage with early OA changes are generally maintained in these subjects.[18] Although it would have been interesting to also examine cartilage from the femoral condyles, these are removed during arthroplasty in several smaller pieces, precluding experimental analysis of the type presented here.

Abbreviations: OA, osteoarthritis; qMRI, quantitative magnetic resonance imaging

Table 1 Distribution of different approaches and of defects

Defect	Approach 1	Approach 2	Medial tibia	Lateral tibia	Patella
3 mm	9	–	3	3	3
5 mm	28	13	14	15	12
8 mm	14	10	9	5	10

Two types of approach were used for creating the defects (table 1).

In 15 specimens (51 defects), the cartilage cylinders inside the punch were removed from the joint plate to create defects as observed, for instance, in osteochondrosis dissecans (approach 1) (fig 1). In nine specimen (23 defects), the cartilage cylinder was left in place and the surrounding cartilage tissue was removed mechanically (approach 2) (fig 2). The actual size of the defects was controlled with a micrometer screw (Hommel Group, Cologne, Germany). For approach 1, the actual diameter of the defects created by the 3 mm punch was 3.08 mm (equivalent to a size of 0.08 cm^2). For the 5 mm punch the exact diameter was 5.06 mm (size = 0.2 cm^2), and for the 8 mm punch the exact diameter was 8.10 mm (size = 0.52 cm^2). For approach 2, the diameter (inside the punch) was 3.96 mm for the 5 mm punch (size = 0.12 cm^2), and 6.44 mm for the 8 mm punch (size = 0.33 cm^2). Owing to the small inner diameter (<1.8 mm) of the 3 mm punch, no reproducible defect size was created and these lesions were thus not included in the analysis.

MR imaging, image analysis, and validation

To achieve high contrast between cartilage and bone, specimens were positioned in a container filled with contrast medium (Lumirem, Guerbet, Roissy, France) during imaging. Gelatin was added, to stabilise the specimens mechanically in the liquid contrast medium (fig 3). In this way the cartilage plates were positioned in the middle of the container, avoiding imaging artefacts that might have occurred at its edges.

A clinical 1.5 T MRI system (Magnetom Sonata, Siemens, Erlangen, Germany) was used, and a T_1 weighted gradient echo sequence with water excitation, which has been previously validated for quantitative cartilage imaging.[17–21] The spatial resolution was 0.31 mm×0.31 mm (in plane) and the slice thickness 1.5 mm. The acquisition time was 9 minutes 50 seconds for each tibial compartment, and 10 minutes 30 seconds for the patella.

After transfer of the image data to a multiprocessing computer (Octane Duo, Silicon Graphics Inc, Mountain View, CA), the cartilage was segmented semiautomatically using a B-spline snake algorithm.[22] The person who performed the image analysis (DA) was unaware of the number of defects for each surface, their position, or their size (diameter).

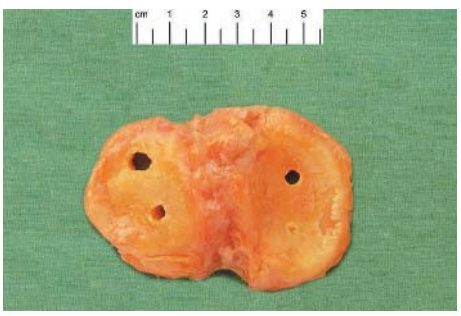

Figure 1 Tibial cartilage plate demonstrating focal defects (two medial, one lateral) created by a cylindrical punch (approach 1).

Figure 2 Patellar cartilage plate demonstrating approach 2, leaving two cartilage cylinders in place, while the surrounding cartilage tissue was removed.

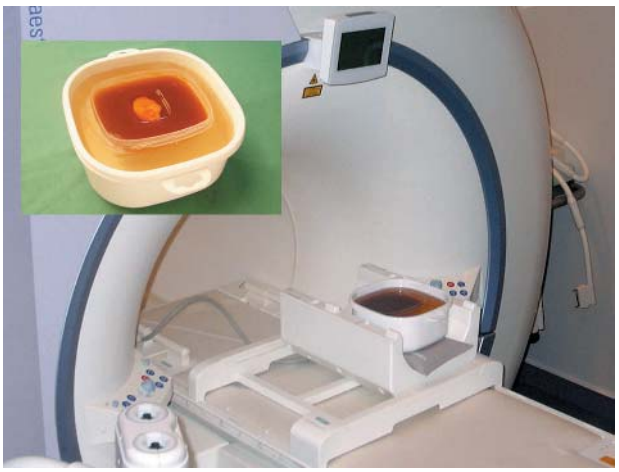

Figure 3 MRI set up. For imaging the joint plates were placed in the middle of a pot being filled with high viscosity solution.

In the next step, the defects themselves (approach 1) were segmented using the same image analysis techniques mentioned above (fig 4). The depth of the defect was defined by the thickness of the cartilage surrounding this tissue.[23] The diameter of the defect was then calculated from the volume of the defect and its depth (thickness of surrounding tissue) using the following formula:

$$r^2 = V/\pi h$$
$$r = \sqrt{r^2}$$
$$d = 2r$$

where h = mean cartilage thickness, V = defect volume.

In approach 2, the remaining cartilage cylinders were segmented directly (fig 5). The same software[23] and procedure was then used to compute the volume and thickness of the cartilage defect and its diameter. This second approach was performed to find out whether the interpolated cartilage/joint and cartilage/bone surface of approach 1 has an influence on the results.

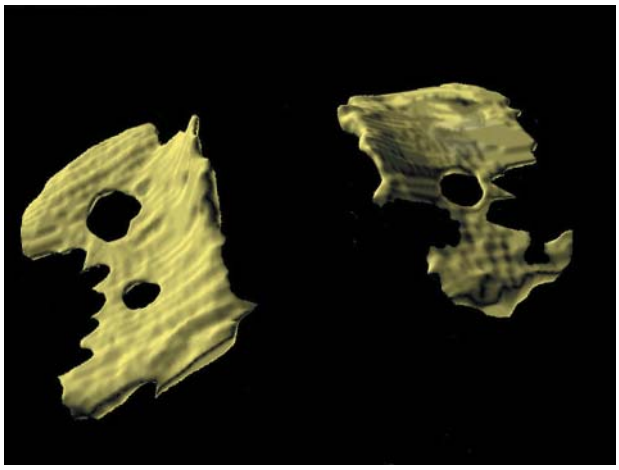

Figure 4 Three dimensional reconstruction of a tibial cartilage plate with two defects medial and one defect lateral formed by approach 1. This image is comparable to the original (fig 1).

Statistics

The systematic (mean deviation) and random pairwise differences (mean over- or underestimation when eliminating the + and − signs) between the actual defect size (as determined with the micrometre screw) and the digital analysis results from the MR images were assessed and evaluated for statistical significance using a paired Student's *t* test. Finally, the data were displayed using a box and whiskers plot (fig 6).

RESULTS

The number and location of all cartilage defects were accurately detected by MRI analysis. This applied to all cartilage plates, all lesion diameters, and both approach 1 and 2.

For approach 1, the accuracy of the MR based measurement technique clearly improved with the size of the defect: Random differences with physical measurements were 1.3 (0.58) mm (±42%) for the 3 mm defects, 1.0 (0.57) mm (±20.7%) and 0.1 (0.39) mm (±3.9%) for the 5 mm and 8 mm defects, respectively. While there was a significant overestimation of defect size with MR imaging in the 3 mm (±42%; $p<0.05$) and 5 mm lesions (±21%; $p<0.05$), no systematic error (±3.9 %; p = NS) was seen for the 8 mm defects (table 2).

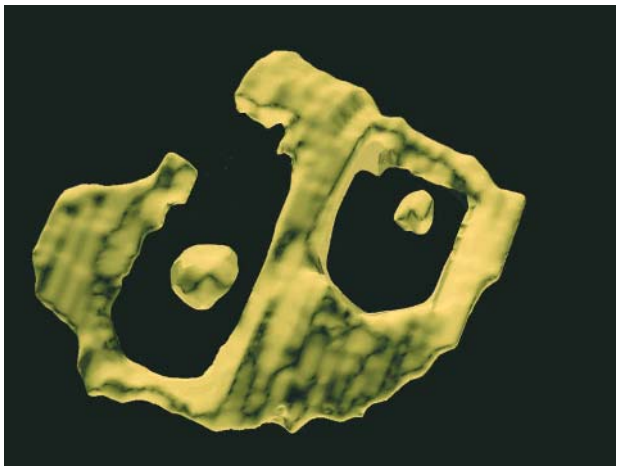

Figure 5 Three dimensional reconstruction of a patellar cartilage plate with two defects formed by approach 2. This image is comparable to the original (fig 2).

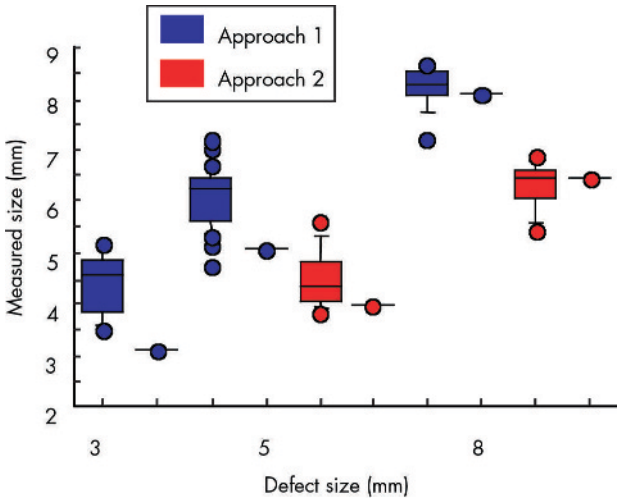

Figure 6 Box and whiskers plot. Chart of results (approaches 1 and 2).

With approach 2, the degree of accuracy was somewhat higher than with approach 1 for 5 mm defects, with random differences amounting to 0.51 (0.53) mm (±13.4%). However, for 8 mm defects the level of accuracy was similar, with random difference amounting to 0.12 (0.45) mm (±5.0%). Although there was a significant overestimation of the defect size in 5 mm defects (±13.4 %; $p<0.05$), there was no significant over- or underestimation with this approach in the 8 mm defects (±5%, p = 0.44) (table 3).

No difference was seen between the joint plates (patella, medial tibia, lateral tibia). In all localisations approach 1 showed smaller differences (0.07–0.34 mm; 8.9–10.7%) than approach 2 (0.62–0.71 mm; 13.3–16.1%), but this difference was not significant.

DISCUSSION

In this study we examined the ability of qMRI to determine accurately focal cartilage lesions of various diameters. Only one previous study has examined these relationships,[24] but those authors examined only patellar defects with diameters of 1–5 mm in elderly donors. Here we show that qMRI yields a high degree of accuracy, at least for larger cartilage defects in patellar, medial tibial, and lateral tibial cartilage, both in normal, healthy cartilage and in early OA cartilage. Although MRI significantly overestimated the small 3 mm defects, the difference was much smaller in the 8 mm defects.

A limitation of this study is that experimental cartilage defects were evaluated and these experimental defects may be structurally different from cartilage defects occurring under real pathophysiological conditions. The results presented here thus need to be confirmed under clinical conditions, but the current data suggest that the approach is promising and displays potential to obtain accurate results in clinical studies. Strengths of the current study are that defects of different sizes were compared systematically, and that the results were obtained in various cartilage plates of the human knee, both in normal and early OA cartilage.

Preoperative quantification of cartilage defects would be very helpful for planning surgical treatment of focal cartilage lesions.[25 26] Defects of a small size are generally treated differently from those of larger size (for example, autologous cartilage transplantation versus mosaicplasty or posterior femur condyle transfer),[3 26] and non-invasive measurement of the actual defect size preoperatively may thus significantly improve presurgical planning. The MRI approach presented

Table 2 Defect size determined by qMRI and real defect size in approach 1. Random and systematic differences for 3, 5, and 8 mm defects

Defect	Real size	Measured size	Difference (mm)	Systematic difference (mm%)	Absolute difference (mm%)
3 mm	3.08	3.87	0.79	25.7	25.7
	3.08	4.57	1.49	48.4	48.4
	3.08	4.47	1.39	45.2	45.2
	3.08	3.51	0.43	13.8	13.8
	3.08	3.66	0.58	18.9	18.9
	3.08	4.33	1.25	40.5	40.5
	3.08	5.18	2.10	68.0	68.0
	3.08	4.80	1.72	55.9	55.9
	3.08	4.96	1.88	61.0	61.0
Mean		4.37	1.29	41.9	41.9
SD		0.58	0.58	19.0	19.0
5 mm	5.06	5.33	0.27	5.4	5.4
	5.06	5.13	0.07	1.4	1.4
	5.06	6.34	1.28	25.2	25.2
	5.06	5.53	0.47	9.2	9.2
	5.06	6.08	1.02	20.2	20.2
	5.06	6.23	1.17	23.2	23.2
	5.06	5.36	0.30	5.9	5.9
	5.06	6.22	1.16	23.0	23.0
	5.06	5.66	0.60	11.9	11.9
	5.06	6.20	1.14	22.5	22.5
	5.06	5.51	0.45	8.8	8.8
	5.06	4.74	−0.32	−6.3	6.3
	5.06	6.48	1.42	28.0	28.0
	5.06	5.90	0.84	16.5	16.5
	5.06	6.21	1.15	22.8	22.8
	5.06	6.65	1.59	31.5	31.5
	5.06	6.33	1.27	25.2	25.2
	5.06	6.48	1.42	28.0	28.0
	5.06	6.27	1.21	23.8	23.8
	5.06	5.82	0.76	15.0	15.0
	5.06	6.72	1.66	32.7	32.7
	5.06	7.18	2.12	41.9	41.9
	5.06	7.02	1.96	38.7	38.7
	5.06	6.23	1.17	23.1	23.1
	5.06	5.43	0.37	7.2	7.2
	5.06	6.63	1.57	31.0	31.0
	5.06	6.29	1.23	24.4	24.4
	5.06	6.40	1.34	26.5	26.5
Mean		6.09	1.03	20.3	20.7
SD		0.58	0.58	11.4	10.3
8 mm	8.10	8.53	0.43	5.4	5.4
	8.10	8.07	−0.03	−0.3	0.3
	8.10	8.38	0.28	3.4	3.4
	8.10	8.43	0.33	4.1	4.1
	8.10	7.79	−0.31	−3.9	3.9
	8.10	8.27	0.17	2.1	2.1
	8.10	8.66	0.56	6.9	6.9
	8.10	8.27	0.17	2.1	2.1
	8.10	7.84	−0.26	−3.3	3.3
	8.10	8.10	0.00	0.0	0.0
	8.10	8.52	0.42	5.2	5.2
	8.10	8.22	0.12	1.4	1.4
	8.10	7.21	−0.89	−11.0	11.0
	8.10	8.51	0.41	5.1	5.1
Mean		8.20	0.10	1.2	3.9
SD		0.39	0.39	4.8	2.9

*$p<0.05$.

here could also help to analyse the efficacy of various therapeutic strategies by non-invasive means, and without requiring an invasive procedure such as arthroscopy.[27] Additionally, it should be mentioned that quantifying focal cartilage defects by arthroscopy has low precision and a high interindividual variability.[28 29]

The overestimation of smaller defects is probably due to the limited pixel resolution of 0.31 mm and inherent partial volume effects. Although higher in-plane resolutions are technically feasible, these inevitably lead to a substantial increase in imaging time, which limits the clinical practicability of the protocols. However, because most of the clinically relevant defects in osteochondrosis dissecans or osteochondral fractures are at least 1 cm^2,[2 6] the accuracy determined with the given resolution and imaging time appears sufficient to measure the size of these defects. Because MRI of articular cartilage at 3.0 T is currently emerging, the improvements of signal to noise and contrast to noise ratios and/or spatial resolution at 3 T may be exploited to improve further the accuracy of focal cartilage defects measurement in the future, without the need for longer imaging times. Although experimental MRI methods for evaluating cartilage composition are currently under development,[30] an established, validated protocol does not yet

Table 3 Defect size determined by qMRI and real defect size in approach 2. Random and systematic differences for 5 and 8 mm defects

Defect	Real size	Measured size	Difference (mm)	Systematic difference (mm%)	Absolute difference (mm%)
5 mm	3.96	4.60	0.64	16.24	16.24
	3.96	4.21	0.25	6.35	6.35
	3.96	4.77	0.81	20.36	20.36
	3.96	4.36	0.40	10.20	10.20
	3.96	3.96	0.00	−0.09	0.09
	3.96	4.33	0.37	9.37	9.37
	3.96	5.25	1.29	32.58	32.58
	3.96	4.22	0.26	6.53	6.53
	3.96	4.05	0.09	2.29	2.29
	3.96	4.85	0.89	22.36	22.36
	3.96	4.05	0.09	2.30	2.30
	3.96	5.62	1.66	42.04	42.04
	3.96	3.83	−0.13	−3.27	3.27
Mean		4.47	0.51	12.86	13.38
SD		0.53	0.53	13.39	12.83
8 mm	6.44	6.38	−0.06	−0.98	0.98
	6.44	5.77	−0.67	−10.33	10.33
	6.44	6.04	−0.40	−6.14	6.14
	6.44	6.90	0.46	7.19	7.19
	6.44	6.68	0.24	3.76	3.76
	6.44	6.52	0.08	1.24	1.24
	6.44	6.41	−0.03	−0.47	0.47
	6.44	5.41	−1.03	−15.93	15.93
	6.44	6.51	0.07	1.04	1.04
	6.44	6.61	0.17	2.58	2.58
Mean		6.32	−0.12	−1.80	4.96
SD		0.45	0.45	7.01	5.03

*$p<0.05$.

exist for the reproducible assessment of a defined component of cartilage for an entire cartilage plate, including evaluation of the adequacy of a graft that plugs a chondral defect or integration of a plug into the surrounding cartilage matrix.

We tested two different techniques for creating focal cartilage defects here: one (approach 1) simulates the clinical situation of osteochondrosis dissecans or osteochondral fractures, where cartilage tissue is lost from the bed. The other technique (approach 2) was used as a control, because in technique 1 the depth of the defect had to be estimated indirectly from the cartilage thickness of the surrounding cartilage tissue. With approach 2, however, we were able to measure the thickness of the cartilage plug directly. As there was no significant difference in the results for the two approaches, this study shows that the estimation of cartilage defect depth from the surrounding tissue is possible, at least under the given experimental conditions.

In this study we demonstrated for the first time that qMRI can be used accurately to measure focal cartilage defects in all compartments of the human knee, if suitable MRI sequences and three dimensional image analysis techniques are applied. The technique presented here may bring about important advances in the diagnostics and presurgical planning of the treatment of focal cartilage defects in OA, osteochondrosis dissecans and osteochondral fractures, and in evaluating the efficacy of different types of treatment.

Authors' affiliations

H Graichen, D Al-Shamari, S Hinterwimmer, R von Eisenhart-Rothe, Research Group for Kinematics and Biomechanics, Orthopaedic Department, University of Frankfurt, Frankfurt, Germany
T Vogl, Institute for Clinical and Interventional Radiology, University of Frankfurt, Frankfurt, Germany
F Eckstein, Institute of Anatomy, Paracelsus Private Medical University, Salzburg, Austria

REFERENCES

1 **Robertson W**, Kelly BT, Green DW. Osteochondritis dissecans of the knee in children. *Curr Opin Pediatr* 2003;**15**:38–44.
2 **Bentley G**, Biant L, Carrington R, Akmal M, Goldberg A, Willia A, *et al*. A prospective, randomised comparison of autologous chondrocyte implantation versus mosaicplasty for osteochondral defects in the knee. *J Bone Joint Surg Br* 2003;**85**:223–30.
3 **Burkart AC**, Schoettle PB, Imhoff AB. Surgical treatment of cartilage damage. *Der Unfallchirurg* 2001;**104**:789–807.
4 **Kocher MS**, Micheli LJ, Yaniv M, Zurakowski D, Ames A, Adrignolo AA. Functional and radiographic outcome of juvenile osteochondritis dissecans of the knee treated with transarticular arthroscopic drilling. *Am J Sports Med* 2001;**29**:562–6.
5 **Peterson L**, Brittberg M, Kiviranta I, Akerlund EL, Lindahl A. Autologous chondrocyte transplantation. Biomechanics and long-term durability. *Am J Sports Med* 2002;**30**:2–12.
6 **Peterson L**, Minas T, Brittberg M, Lindahl A. Treatment of osteochondritis dissecans of the knee with autologous chondrocyte transplantation: results at two to ten years. *J Bone Joint Surg Am* 2003;**85**:17–24.
7 **Hangody L**, Füles P. Autologous osteochondral mosaicplasty for the treatment of full-thickness defects of weight-bearing joints. *J Bone Joint Surg Am* 2003;**85**:25–32.
8 **Bruns J**, Steinhagen J. Treatment of deep hyalin cartilage defects with autologous perichondrial grafts. *Int J Sports Med* 2003;**24**:382–8.
9 **Shasha N**, Krywulak S, Backstein D, Pressmann A, Gross AE. Long-term follow-up of fresh tibial osteochondral allografts for failed tibial plateu fractures. *J Bone Joint Surg Am* 2003;**85**:33–9.
10 **Buckland-Wright C**. Radiographic assessment of osteoarthritis: comparison between existing methods. *Osteoarthritis Cartilage* 1999;**7**:430–3.
11 **Linden B**, Jonsson K, Redlund-Johnell I. Osteochondritis dissecans of the hip. *Acta Radiol* 2003;**44**:67–71.
12 **Poole AR**. What type of cartilage repair are we attempting to obtain? *J Bone Joint Surg Am* 2003;**85**(suppl 2):40–4.
13 **Loredo R**, Sanders TG. Imaging of osteochondral injuries. *Clin Sports Med* 2001;**20**:249–78.
14 **O'Connor MA**, Palaniappan M, Khan N, Bruce CE. Osteochondritis dissecans of the knee in children. A comparison of MRI and arthroscopic findings. *J Bone Joint Surg Br* 2002;**84**:258–62.
15 **Link TM**, Lindner N, Haeussler M, Reimer P, Allkemper T, Jerosch J, *et al*. Artificially produced cartilage lesions in small joints: detection with optimized MRI-sequences. *Magn Reson Imaging* 1997;**15**:949–56.
16 **Link TM**, Majumdar S, Peterfy C, Daldrup HE, Uffmann M, Dowling C, Steinbach L, Genant HK. High resolution MRI of small joints: impact of spatial resolution on diagnostic performance and SNR. *Magn Reson Imaging* 1998;**16**:147–55.

17 **Burgkart R**, Glaser C, Hylik-Dürr A, Englmeier KH, Reiser M, Eckstein F. Magnetic resonance imaging-based assessment of cartilage loss in severe osteoarthritis. Accuracy, precision and diagnostic value. *Arthritis Rheum* 2001;**44**:2072–7.
18 **Graichen H**, von Eisenhart-Rothe R, Vogl T, Englmeier KH, Eckstein F. Quantitative assessment of cartilage status in osteoarthritis by quantitative magnetic resonance imaging: technical validation for use in analysis of cartilage volume and further morphologic parameters. *Arthritis Rheum* 2004;**50**:811–6.
19 **Glaser C**, Faber S, Eckstein F, Fischer H, Springer V, Heudorfer L, *et al*. Optimization and validation of a rapid high-resolution T1-w 3D FLASH water excitation MRI sequence for the quantitative assessment of articular cartilage volume and thickness. *Magn Reson Imaging* 2001;**19**:177–85.
20 **Graichen H**, Springer V, Flamann T, Stammberger T, Glaser C, Englmeier KH, *et al*. High-resolution, selective water-excitation MR imaging for quantitative assessment of thin cartilage layers: validation with CT-arthrography and A-mode ultrasound. *Osteoarthritis Cartilage* 2000;**8**:106–14.
21 **Graichen H**, Jakob J, von Eisenhart-Rothe R, Englmeier KH, Reiser M, Eckstein F. Validation of cartilage volume and thickness measurements in the human shoulder with quantitative magnetic resonance imaging (qMRI). *Osteoarthritis Cartilage* 2003;**11**:475–82.
22 **Stammberger T**, Eckstein F, Michaelis M, Englmeier KH, Reiser M. Interobserver reproducibility of quantitative cartilage measurements: comparison of B-spline snakes and manuell segmentation. *Magn Reson Imaging* 1999;**17**:1033–42.
23 **Stammberger T**, Eckstein F, Englmeier KH, Reiser M. Determination of 3D cartilage thickness data from MR imaging: computational method and reproducibility in the living. *Magn Reson Med* 1999;**41**:529–36.
24 **McGibbon CA**, Trahan CA. Measurement accuracy of focal cartilage defects from MRI and correlation of MRI graded lesions with histology: a preliminary study. *Osteoarthritis Cartilage* 2003;**11**:483–93.
25 **Burstein D**, Gray M. New MRI techniques for imaging cartilage. *J Bone Joint Surg Am* 2003;**85**:70–7.
26 **McCauley TR**, Disler DG. Magnetic resonance imaging of articular cartilage of the knee. *J Am Acad Orthop Surg* 2001;**9**:2–8.
27 **Raynauld JP**. Quantitative magnetic resonance imaging of articular cartilage in knee osteoarthrits. *Curr Opin Rheumatol* 2003;**15**:647–50.
28 **Oakley SP**, Portek I, Szomor Z, Turnbull A, Murrell GA, Kirkham BW, *et al*. Accuracy and reliability of arthroscopic estimates of cartilage lesion size in a plastic knee simulation model. *Arthroscopy* 2003;**193**:282–9.
29 **Schafer D**, Boss A, Hintermann B. Accuracy of arthroscopic assessment of anterior ankle cartilage lesions. *Foot Ankle Int* 2003;**24**:317–20.
30 **Wayne JS**, Kraft KA, Shields KJ, Yin C, Owen JR, Disler DG. MR imaging of normal and matrix-depleted cartilage: correlation with biomechanical function and biochemical composition. *Radiology* 2003;**228**:493–9.